



www.sciencemag.org/cgi/content/full/science.1219330/DC1

Supporting Online Material for

Energy Capture from Thermolytic Solutions in Microbial Reverse-Electrodialysis Cells

Roland D. Cusick, Younggy Kim, Bruce E. Logan*

*To whom correspondence should be addressed. E-mail: blogan@psu.edu

Published 1 March 2012 on *Science Express*

DOI: 10.1126/science.1219330

This PDF file includes:

Materials and Methods

Figs S1 to S7

References (30–36)

Materials and Methods

Reactor Construction. The lab scale MRC reactor was constructed as previously described (13) with minor modifications (Fig. 1). The 4-cm cubic anode chamber (Lexan, 30 mL empty bed volume) contained a graphite brush anode ($D = 2.7$ cm, $L = 2.3$ cm, 0.22 cm² projected area based on all fibers in the brush; Mill-Rose Labs Inc., OH). The brush anode was heat treated (30) before it was inoculated with the effluent from an existing MFC and enriched in a conventional single chamber MFC prior to MRC operation. The cathode chamber (2-cm cubic chamber, 18 mL empty bed volume) contained a 7-cm² (projected surface area) air cathode with a Pt catalyst (0.5 mg Pt/cm²) applied on a carbon cloth as previously described (31), with a Nafion catalyst binder (water side) and four layers of polytetrafluoroethylene diffusion layers (air side). Although Pt was used as a catalyst here in order to benchmark performance against previously tested systems using NaCl solutions (13), nearly identical cathode performance has been obtained using activated carbon catalysts instead of Pt catalysts in microbial fuel cells (32). The cathode chamber also served as the first flow channel of the high concentrate salt stream to prevent the pH rise in the cathode chamber.

The RED stack, assembled between the anode and cathode chambers, consists of with 6 anion- and 5 cation-exchange membranes (Selemion AMV and CMV, Asahi glass, Japan), creating 5 pairs of alternating HC and LC chambers as previously described (13). Inter-membrane chambers were sealed and separated by silicon gaskets, each with an 8-cm² (2×4 cm) rectangular cross section cut out. Inter-membrane chamber width (1.3 mm) was maintained with a 2 cm² (0.5×4 cm) strip of polyethylene mesh. The total ion exchange membrane area in the RED stack was 88 cm². The total MRC empty bed

volume was 58.4 mL (RED stack + Cathode = 28.4 mL; Anode = 30 mL). The HC solution entered the cathode chamber and flowed serially through the 5 HC cells in the stack, exiting from the cell next to the anode chamber (Fig. 1). The LC stream entered the RED stack near the anode and flowed serially through the 5 LC cells in the stack, exiting from the cell next to the cathode chamber. A peristaltic pump (Cole Parmer, IL) continuously fed the HC and LC solutions at a flow rate of 1.6 mL/min, unless specified otherwise.

After stable performance in the MRC, the working electrodes (anode and cathode) were transferred to a cubic 4-cm (30 mL empty bed volume) single chamber MFC reactors to establish a performance baseline.

Peak power, maximum energy recovery, and energy efficiency of the MRC and MFC were determined in separate experiments. During power density curve experiments fresh HC solution was pumped through the RED stack with the effluent collected in separate reservoirs. To maximize energy recovery and energy efficiency, 0.1-L HC and LC solutions were recycled in airtight flow paths for the duration of anode feeding cycles over a batch recycle experiment. Before each batch the stack and tubing were flushed with matching solutions.

Solutions. Ammonium bicarbonate HC solutions were prepared by dissolving ammonium bicarbonate salt (Alfa Aesar, MA) into deionized water within an airtight vessel. The initial HC solutions tested were 1.8, 1.1, 0.95, 0.8, and 0.5 M. The LC solutions were prepared to produce salinity ratios of 50, 100, and 200 by diluting an aliquot of the HC solution. The anode solutions contained 1 g/L of sodium acetate (organic substrate for exoelectrogenic bacteria growing on anode), in 50 mM carbonate

buffer (4.2 g/L NaHCO_3^-) containing 0.231 g/L $\text{NH}_4\text{H}_2\text{PO}_4$ and trace vitamins and minerals (33). Domestic wastewater was collected from the primary clarifier of the Penn State University wastewater treatment plant. The cathode contained ammonium bicarbonate HC solution, therefore protons for oxygen reduction at the cathode were provided by ammonium and bicarbonate ions as well as water dissociation.

A second order relationship between ammonium bicarbonate solution concentration and solution conductivity (determined by conducting a stepwise dilution series) was used to estimate initial and final concentrations of HC and LC streams. Conductivity and pH of the HC and LC streams were measured (Mettler-Toledo, OH) before and after each batch recycle experiment.

Analysis. Power production in batch recycle experiments was determined by measuring the potential drop across a fixed external resistance (300 Ω) for both MRC and single chamber MFC operations. Voltage drop was recorded every 20 minutes by a digital multimeter (Keithley Instruments, OH). Electrical current (i) was determined by Ohm's law. Power was calculated by multiplying the electrical current and total cell voltage. Reported power densities were based on the cathode projected area (7 cm^2). To determine the maximum MRC power (P_{MRC}) production at each condition the reactor was held at open circuit voltage for one hour and then the external resistance was decreased from 1,000 to 50 Ω every 20 minutes with the voltage recorded at each resistance. Power contribution by the electrode reactions (P_{MFC}) was determined by measuring the anode potential (E_{an}) and cathode potential (E_{cat}) against Ag/AgCl reference electrodes (BASi, IN): $P_{MFC} = (E_{cat} - E_{an}) \times i$. The RED stack power contribution was calculated by finding

stack voltage (V_{stk}) with two reference electrodes located on both ends of the stack as:

$$P_{RED} = V_{stk} \times i.$$

The MRC anode was transferred to a single chamber MFC to determine baseline power production in fed-batch experiments. In the single chamber MFC, same substrate solutions (sodium acetate in carbonate buffer solution and domestic wastewater) were provided to determine peak power production.

Coulombic efficiency was determined as previously described (34). Energy recovery (r_E) is defined by the ratio of energy produced by the MRC reactor and the energy input as substrate and salinity gradient as written in Eq. (1). Energy efficiency (η_E) was calculated as the ratio of energy produced to the energy consumed based on the substrate used and the salinity gradient, according to (13):

$$r_E = \frac{E_{MRC}}{n_{s,0} \Delta G_s + \Delta G_{mix,0}} \cdot 100\% \quad (1)$$

$$\eta_E = \frac{E_{MRC}}{(n_{s,0} - n_{s,f}) \Delta G_s + (\Delta G_{mix,0} - \Delta G_{mix,f})} \cdot 100\% \quad (2)$$

where E_{MRC} is the energy produced per batch (kJ), n_s is the moles of substrate (acetate) initially fed to the anode (0) and at the end of the batch cycle (f), and ΔG_s is the Gibb's free energy of substrate [acetate = -846.6 kJ/mol (35), domestic wastewater = 17.8 kJ/g-COD (36)]. ΔG_{mix} is the free energy that can be created by mixing of HC and LC solutions until the two solutions reach equilibrium concentration, calculated as:

$$\Delta G_{mix} = RT \sum_i \left(V_{HC} c_{i,HC} \ln \frac{a_{i,mix}}{a_{i,HC}} + V_{LC} c_{i,LC} \ln \frac{a_{i,mix}}{a_{i,LC}} \right) \quad (3)$$

where R is the ideal gas constant (8.314 J/mol-K), T is solution temperature, V is the volume of solution, c is the molar concentration of ionic species i in the solution, and a is the activity of species i in the solution.

At a neutral pH, concentrated ammonium bicarbonate is dominated by ammonium (NH_4^+) and bicarbonate (HCO_3^-) ions, but significant amounts of carbamate (NH_4CO_3^-) and carbonate (CO_3^{2-}) also contribute to ionic strength. Species specific concentrations and activities were estimated with OLI Stream Analysis software (OLI Systems, Inc., Morris Plains, NJ) at a pH of 7 and temperature of 25 °C.

To determine ammonia transport into the anode, total ammonia nitrogen (TAN = NH_3 + NH_4^+) concentration in the substrate was estimated before and after each fed-batch cycle (HACH, Loveland, CO) (31). Based on observed pH, corresponding free ammonia concentration (NH_3) was calculated by:

$$[\text{NH}_3] = [\text{TAN}] \left(1 + \frac{10^{-\text{pH}}}{10^{-\text{pK}_a}} \right)^{-1} \quad (4)$$

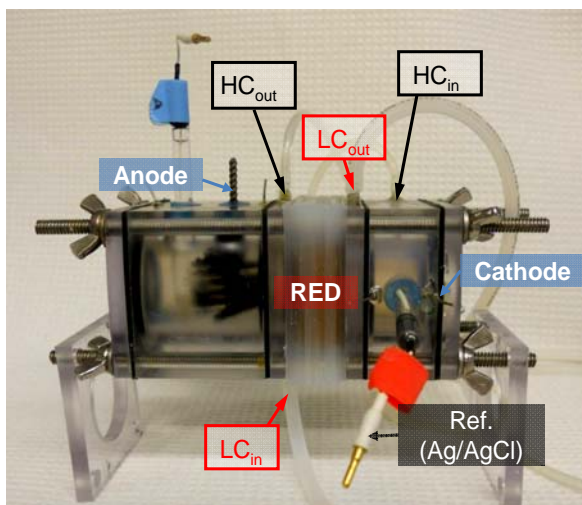


Fig. S1.

Labeled picture of an MRC reactor showing positions of the working (anode and cathode) and reference (Ag/AgCl) electrodes, the RED membrane stack, as well as high (HC) and low concentrate (LC) salt solution influent and effluent ports.

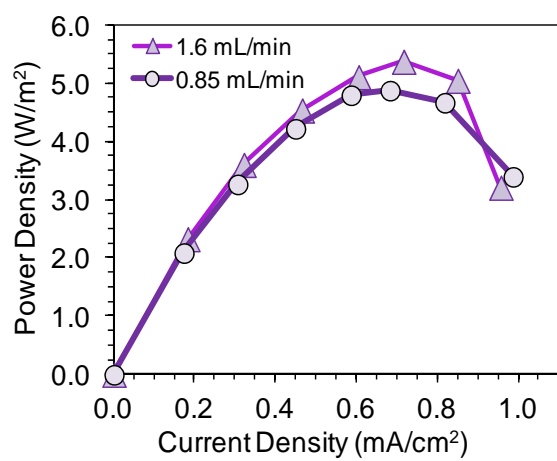


Fig. S2

Power density curves of the MRC (HC = 0.95 M, SR = 100) at different salt solution flow rates.

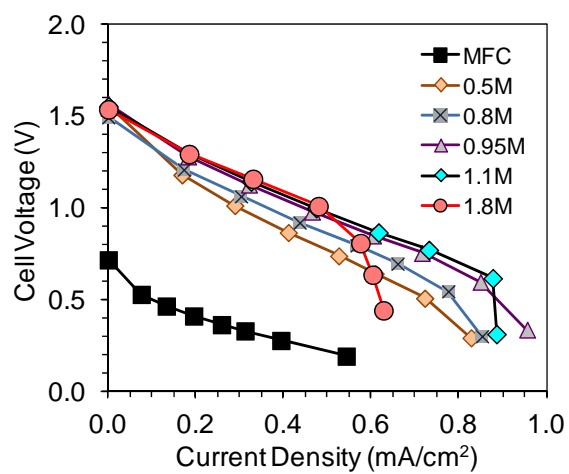


Fig. S3

Polarization curves of the MRC using different HC salt solutions, compared to that of an MFC.

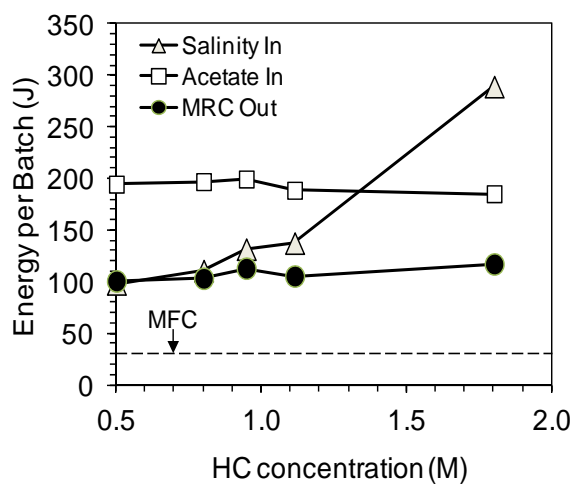


Fig. S4

MRC energy input (acetate and salinity energy) and output at different HC concentrations.

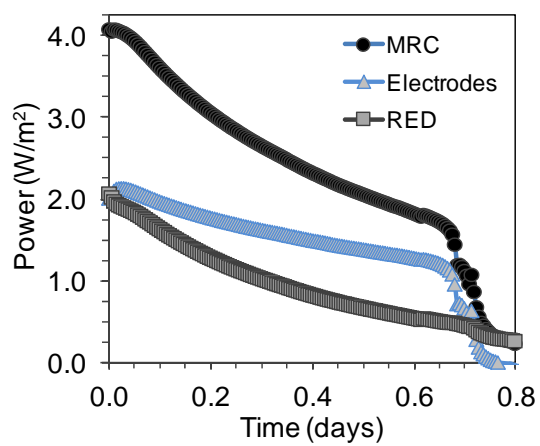
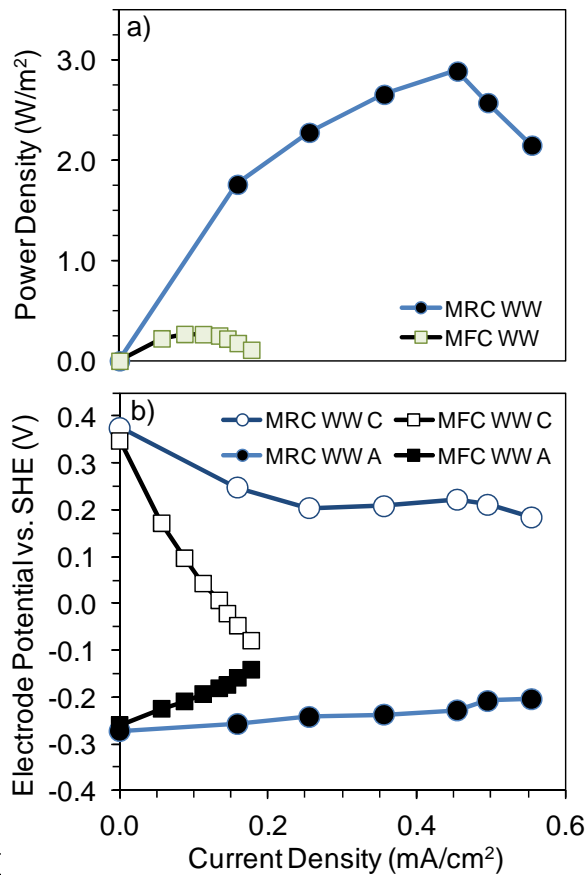
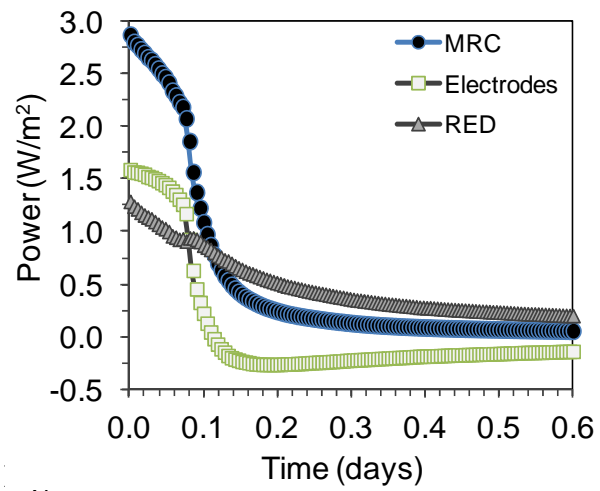


Fig. S5

Batch recycle component (MFC electrodes, RED and total MRC) power profile of MRC fed acetate operating at an external resistance of 300Ω .



a) Peak power density and b) anode (A) and cathode potentials (C) of MRC and single chamber MFC fed domestic wastewater. Notice that the anode and cathode potentials remained relatively constant over the range of current densities. The relatively constant potential indicates that the power performance is stable, suggesting that the system could easily sustain higher power densities with higher organic matter concentrations in the wastewater.



Batch recycle component (Electrodes, RED and total MRC) power profile of MRC fed domestic wastewater operating at an external resistance of 300Ω .

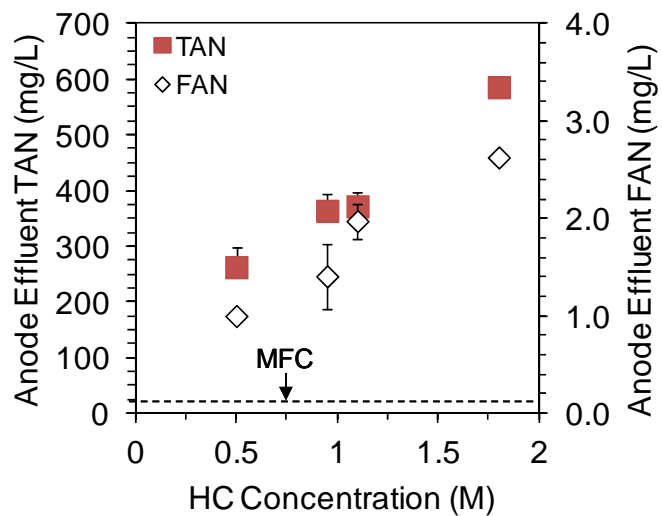


Fig. S7

Ammonia transport into anode chamber at various HC concentrations. The MRC anode effluent concentrations of total ammonia-nitrogen (TAN, $\text{NH}_4^+ + \text{NH}_3$) and free ammonia-nitrogen (FAN, NH_3) were appreciably higher than the single chamber MFC (TAN = 24 ± 5 mg/L, FAN = 0.16 ± 0.02 mg/L).

References and Notes

1. IPCC, Climate Change 2007: Synthesis Report. (IPCC, Geneva, 2007).
2. H. Liu, R. Ramnarayanan, B. E. Logan, Production of electricity during wastewater treatment using a single chamber microbial fuel cell. *Environ. Sci. Technol.* **38**, 2281 (2004). [doi:10.1021/es034923g](https://doi.org/10.1021/es034923g) [Medline](#)
3. R. D. Cusick, P. D. Kiely, B. E. Logan, A monetary comparison of energy recovered from microbial fuel cells and microbial electrolysis cells fed winery or domestic wastewaters. *Int. J. Hydrogen Energy* **35**, 8855 (2010). [doi:10.1016/j.ijhydene.2010.06.077](https://doi.org/10.1016/j.ijhydene.2010.06.077)
4. B. E. Logan *et al.*, Microbial fuel cells: methodology and technology. *Environ. Sci. Technol.* **40**, 5181 (2006). [doi:10.1021/es0605016](https://doi.org/10.1021/es0605016) [Medline](#)
5. B. E. Logan, Exoelectrogenic bacteria that power microbial fuel cells. *Nat. Rev. Microbiol.* **7**, 375 (2009). [doi:10.1038/nrmicro2113](https://doi.org/10.1038/nrmicro2113) [Medline](#)
6. Y. Fan, H. Hu, H. Liu, Sustainable power generation in microbial fuel cells using bicarbonate buffer and proton transfer mechanisms. *Environ. Sci. Technol.* **41**, 8154 (2007). [doi:10.1021/es071739c](https://doi.org/10.1021/es071739c) [Medline](#)
7. Y. Ahn, B. E. Logan, Effectiveness of domestic wastewater treatment using microbial fuel cells at ambient and mesophilic temperatures. *Bioresour. Technol.* **101**, 469 (2010). [doi:10.1016/j.biortech.2009.07.039](https://doi.org/10.1016/j.biortech.2009.07.039) [Medline](#)
8. H. Liu, B. E. Logan, Electricity generation using an air-cathode single chamber microbial fuel cell in the presence and absence of a proton exchange membrane. *Environ. Sci. Technol.* **38**, 4040 (2004). [doi:10.1021/es0499344](https://doi.org/10.1021/es0499344) [Medline](#)
9. S. Cheng, H. Liu, B. E. Logan, Increased power generation in a continuous flow MFC with advective flow through the porous anode and reduced electrode spacing. *Environ. Sci. Technol.* **40**, 2426 (2006). [doi:10.1021/es051652w](https://doi.org/10.1021/es051652w) [Medline](#)
10. G. L. Wick, Power from salinity gradients. *Energy* **3**, 95 (1978). [doi:10.1016/0360-5442\(78\)90059-2](https://doi.org/10.1016/0360-5442(78)90059-2)
11. J. W. Post *et al.*, Salinity-gradient power: Evaluation of pressure-retarded osmosis and reverse electrodialysis. *J. Membr. Sci.* **288**, 218 (2007). [doi:10.1016/j.memsci.2006.11.018](https://doi.org/10.1016/j.memsci.2006.11.018)
12. G. Z. Ramon, B. J. Feinberg, E. M. V. Hoek, Energy. *Environ. Sci.* **4**, 4423 (2011).
13. Y. Kim, B. E. Logan, Microbial reverse electrodialysis cells for synergistically enhanced power production. *Environ. Sci. Technol.* **45**, 5834 (2011). [doi:10.1021/es200979b](https://doi.org/10.1021/es200979b) [Medline](#)
14. Y. Kim, B. E. Logan, Hydrogen production from inexhaustible supplies of fresh and salt water using microbial reverse-electrodialysis electrolysis cells. *Proc. Natl. Acad. Sci. U.S.A.* **108**, 16176 (2011). [doi:10.1073/pnas.1106335108](https://doi.org/10.1073/pnas.1106335108) [Medline](#)
15. R. L. McGinnis, J. R. McCutcheon, M. Elimelech, A novel ammonia-carbon dioxide osmotic heat engine for power generation. *J. Membr. Sci.* **305**, 13 (2007). [doi:10.1016/j.memsci.2007.08.027](https://doi.org/10.1016/j.memsci.2007.08.027)

16. T. Kim *et al.*, Systematic approach for draw solute selection and optimal system design for forward osmosis desalination. *Desalination* **284**, 253 (2012).
[doi:10.1016/j.desal.2011.09.008](https://doi.org/10.1016/j.desal.2011.09.008)
17. J. R. Kim, S. Cheng, S.-E. Oh, B. E. Logan, Power generation using different cation, anion, and ultrafiltration membranes in microbial fuel cells. *Environ. Sci. Technol.* **41**, 1004 (2007). [doi:10.1021/es062202m](https://doi.org/10.1021/es062202m) [Medline](#)
18. X. Xie *et al.*, Energy. *Environ. Sci.* **5**, 5265 (2012).
19. P. L. McCarty, J. Bae, J. Kim, Domestic wastewater treatment as a net energy producer—can this be achieved? *Environ. Sci. Technol.* **45**, 7100 (2011). [Medline](#)
20. B. E. Logan, S. W. Hermanowicz, D. S. Parker, *J. Water Pollut. Control Fed.* **59**, 1029 (1987).
21. D. Parker, J. Bratby, Review of Two Decades of Experience with TF/SC Process. *J. Environ. Eng.* **127**, 380 (2001). [doi:10.1061/\(ASCE\)0733-9372\(2001\)127:5\(380\)](https://doi.org/10.1061/(ASCE)0733-9372(2001)127:5(380))
22. J. Y. Nam, H. W. Kim, H. S. Shin, Ammonia inhibition of electricity generation in single-chambered microbial fuel cells. *J. Power Sources* **195**, 6428 (2010).
[doi:10.1016/j.jpowsour.2010.03.091](https://doi.org/10.1016/j.jpowsour.2010.03.091)
23. B. E. Logan, Extracting hydrogen and electricity from renewable resources. *Environ. Sci. Technol.* **38**, 160A (2004). [doi:10.1021/es040468s](https://doi.org/10.1021/es040468s) [Medline](#)
24. I. Shizas, D. M. Bagley, Experimental Determination of Energy Content of Unknown Organics in Municipal Wastewater Streams. *J. Energy Eng.* **130**, 45 (2004).
[doi:10.1061/\(ASCE\)0733-9402\(2004\)130:2\(45\)](https://doi.org/10.1061/(ASCE)0733-9402(2004)130:2(45))
25. E. Lalaurette, S. Thammannagowda, A. Mohagheghi, P.-C. Maness, B. E. Logan, Hydrogen production from cellulose in a two-stage process combining fermentation and electrohydrogenesis. *Int. J. Hydrogen Energy* **34**, 6201 (2009).
[doi:10.1016/j.ijhydene.2009.05.112](https://doi.org/10.1016/j.ijhydene.2009.05.112)
26. F. Rezaei *et al.*, *Appl. Environ. Microbiol.* **192**, 304 (2009).
27. A. Wang *et al.*, Integrated hydrogen production process from cellulose by combining dark fermentation, microbial fuel cells, and a microbial electrolysis cell. *Bioresour. Technol.* **102**, 4137 (2011). [doi:10.1016/j.biortech.2010.10.137](https://doi.org/10.1016/j.biortech.2010.10.137) [Medline](#)
28. U. S. DOE, Biomass as feedstock for a bioenergy and bioproducts industry: the technical feasibility of a billion-ton annual supply. *DOE/GO-102005-2135* (2005).
29. U. S. EIA, Annual Energy Review 2010. *DOE/EIA-0384* (2010).
30. X. Wang *et al.*, Use of carbon mesh anodes and the effect of different pretreatment methods on power production in microbial fuel cells. *Environ. Sci. Technol.* **43**, 6870 (2009).
[doi:10.1021/es900997w](https://doi.org/10.1021/es900997w) [Medline](#)
31. S. Cheng, H. Liu, B. E. Logan, Increased performance of single-chamber microbial fuel cells using an improved cathode structure. *Electrochem. Commun.* **8**, 489 (2006).
[doi:10.1016/j.elecom.2006.01.010](https://doi.org/10.1016/j.elecom.2006.01.010)

32. F. Zhang, S. Cheng, D. Pant, G. V. Bogaert, B. E. Logan, Power generation using an activated carbon and metal mesh cathode in a microbial fuel cell. *Electrochem. Commun.* **11**, 2177 (2009). [doi:10.1016/j.elecom.2009.09.024](https://doi.org/10.1016/j.elecom.2009.09.024)
33. J. R. Ambler, B. E. Logan, Evaluation of stainless steel cathodes and a bicarbonate buffer for hydrogen production in microbial electrolysis cells using a new method for measuring gas production. *Int. J. Hydrogen Energy* **36**, 160 (2011). [doi:10.1016/j.ijhydene.2010.09.044](https://doi.org/10.1016/j.ijhydene.2010.09.044)
34. H. Liu, S. Cheng, B. E. Logan, Power generation in fed-batch microbial fuel cells as a function of ionic strength, temperature, and reactor configuration. *Environ. Sci. Technol.* **39**, 5488 (2005). [doi:10.1021/es050316c](https://doi.org/10.1021/es050316c) [Medline](#)
35. R. A. Rozendal, H. V. M. Hamelers, K. Rabaey, J. Keller, C. J. N. Buisman, Towards practical implementation of bioelectrochemical wastewater treatment. *Trends Biotechnol.* **26**, 450 (2008). [doi:10.1016/j.tibtech.2008.04.008](https://doi.org/10.1016/j.tibtech.2008.04.008) [Medline](#)
36. E. S. Heidrich, T. P. Curtis, J. Dolfing, Determination of the internal chemical energy of wastewater. *Environ. Sci. Technol.* **45**, 827 (2011). [doi:10.1021/es103058w](https://doi.org/10.1021/es103058w) [Medline](#)